Supplementary Materials

Polypyrrole-coated Fe_2O_3 nanotubes constructed by nanoneedles as high-performance anodes for aqueous asymmetric supercapacitors

Kai Le[a], Mengjiao Gao[b], Dongmei Xu[a], Zhou Wang[b], Guanwen Wang[b],

Wei Liu [a,*], Fenglong Wang [b,c,*], Jiurong Liu [b,*]

[a] State Key Laboratory of Crystal Materials, Institute of Crystal Materials，Shandong University, Shandong 250100, China

[b] School of Materials Science and Engineering, Shandong University, Jinan, Shandong 250061, China

[c] Shenzhen Research Institute of Shandong University, Shenzhen, Guangdong, China

*Corresponding author.

E-mail: weiliu@sdu.edu.cn (W. L.), and jrliu@sdu.edu.cn (J. L.)

Fabrication of ZnO nanorods on Ni foam. The ZnO nanorods were coated on the Ni foam by a wet chemical process according to the previous report with slight modification.[1] Briefly, a seed layer was first formed on carbon cloth by immersing clean Ni foam in 0.5 M $KMnO_4$ for 30 min. A volume of 80 mL solution containing 1.2 mmol of zinc acetate dihydrate, 1.2 mmol of hexamethylenetetramine (HMT), and 3.2 mL of aqueous ammonia (28%) was prepared and stirred at room temperature for 30 min. Subsequently, the above solution was transferred into a 100 mL Teflon-lined stainless steel autoclave with a piece of seeded Ni foam and then hydrothermally reacted at 90 ℃ for 12 h. The obtained substrate was washed with deionized water and dried at 60 ℃.

Fabrication of MnO_2 nanotubes on Ni foam. Firstly, the MnO_2 were deposited on ZnO nanorods by immersing the ZnO nanorods into a 0.03 M $KMnO_4$ aqueous solution (60 mL) in a 100 mL Teflon-lined stainless steel autoclave for hydrothermal treatment under 180 ℃ for 24 h. After the reaction, the substrate was washed with deionized water and dried at 60 ℃. Subsequently, the substrate was immersed into 2 M KOH aqueous solution for 6 h to remove ZnO template. After the etching progress, well-aligned MnO_2 nanotubes on the Ni foam were obtained. The weighed mass of MnO_2 nanotube is about 1.1 mg cm^{-2}

Fabrication of Fe_2O_3 nanotubes on Ni foam. The obrained MnO_2 nanotubes sample was employed as the sacrificed template to synthesis the Fe_2O_3 nanotubes by a previously reported method with slight modification.[2] Briefly, 105 mg of $FeSO_4 \cdot 7H_2O$ was dissolved in 60 mL of mixed ethylene glycol and deionized water (v/v = 1/7). After stirring for about 10 min, this translucent solution and the as-prepared MnO_2 nanotubes substrate were both transferred into a 100 mL Teflon-lined stainless steel autoclave for hydrothermal treatment under 120 ℃ for 45 min. After cooling naturally to room temperature, the Ni foam with iron hydroxides were taken out and rinsed thoroughly with deionized water and then dried at 60 ℃. The Fe_2O_3 nanotubes were obtained by annealing the as-prepared iron hydroxide product at 450 ℃ in air for 1h with a heating rate of 1 ℃ min^{-1}. The loading mass of Fe_2O_3 nanotubes on nickel foam is about 1.0 mg cm^{-2}.

Fabrication of Fe_2O_3@PPy nanotubes on Ni foam. PPy was coated on Fe_2O_3 nanotubes by a facile

polymerization method. Typically, 0.1 mL pyrrole, 0.274 g p-toluenesulfonic acid monohydrate ($PTsOH \cdot H_2O$) were dispersed in 60 mL of deionized water and stirred for 30 min. Then, a piece of as-prepared Fe_2O_3 nanotubes substrate was immersed in solution. Subsequently, 0.330 g ammonium persulphate which was dissolved in 20 mL of deionized water was added dropwise to the above solution with cooling in an ice-water bath. The mixture was then stirred for 60 min. Finally, the Fe_2O_3@PPy nanotubes was obtained and dried at 60 ℃ for 12 h after washing by deionized water and ethanol. The estimated loading of Fe_2O_3@PPy nanotubes is around 1.3 mg cm^{-2}.

Assembly of asymmetric supercapacitors (ASCs). The ASC devices were fabricated using Fe_2O_3@PPy nanotubes as anode, MnO_2 nanotubes as cathode, and 1 M Na_2SO_4 as electrolyte. Typically, the anode and cathode were directly immersed into 1 M Na_2SO_4 solution.

Materials Characterizations. X-ray powder diffractions (XRD) were conducted using the Rigaku DMax-RC X-ray diffractometer to analyze the crystallization of as-prepared samples. Scanning electron microscope (SEM) images and energy dispersive X-ray spectroscopy (EDX) mapping images were obtained using the field-emission scanning electron microscope (FE-SEM, JEOL, JSM-6700F, 10 kV). The morphology and microstructure of the samples was investigated by using the high-resolution transmission electron microscope (HR-TEM, JEOL, JEM-2100, 200 kV). The X-ray photoelectron spectrum (XPS) of as-prepared sample was recorded using Kratos Analytical spectrometer to determine the surface properties.

Electrochemical measurements. The electrochemical performances of as-made working electrodes were first characterized by cyclic voltammogram (CV), galvanostatic charge-discharge (GCD) and electrochemical impedance spectra (EIS) on an Iviumstat electrochemistry workstation in three-electrode system including a Pt foil counter electrode, a Ag/AgCl reference electrode, and 1 M Na_2SO_4 aqueous electrolyte.

Then, the electrochemical performances of as-assembled ASCs were also investigated using an Iviumstat electrochemistry workstation in two-electrode system. The EIS spectra were measured in the frequency from

10 to 0.01 KHz at an open circuit potential of around 0.25 V.

The specific capacitances of single electrode can be determined from GCD curves through formula (1):[3]

$$C = \frac{I \times \Delta t}{m \times \Delta V} \tag{1}$$

where Δt, I, and ΔV are the discharge time, the charge-discharge current, and the potential range excluding IR drop in charge-discharge curves, and m represents the mass loading of the working electrode.

For the ASC device, taking into account the charge storage performances of cathode and anode, the mass ration of two electrodes was determined by equation:[4]

$$\frac{m_+}{m_-} = \frac{C_- \Delta V_-}{C_+ \Delta V_+} \tag{2}$$

where *m*, *V*, and *C* represents the mass loading, potential range and specific capacitance of cathode (+) and anode (-), respectively. The specific capacitance, energy density, and power density of ASC device were calculated by formulas:[5]

$$C_{cell} = \frac{I \times \Delta t}{m \times \Delta V} \tag{3}$$

$$E = \frac{1}{2} C_{cell} \Delta V^2 \tag{4}$$

$$P = \frac{E}{\Delta t} \tag{5}$$

where C_{cell}, ΔV, and Δt are the corresponding parameters in discharge curves, and m represents the total mass loading of two electrode in ASC device.

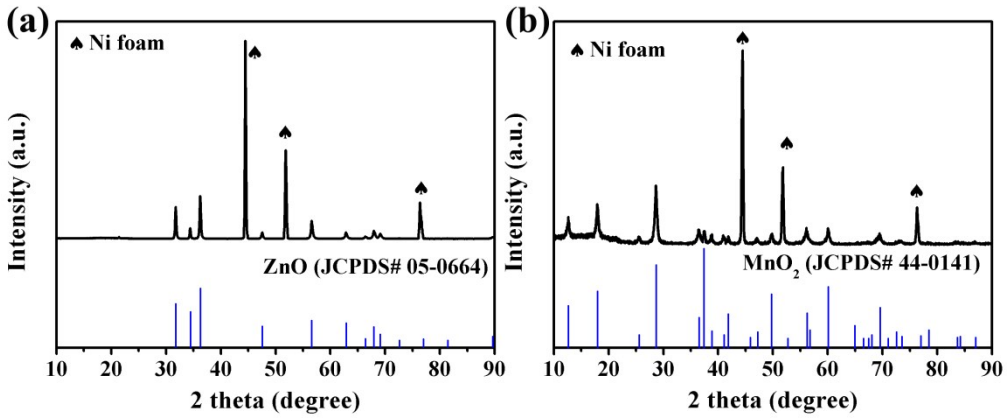

Figure S1. XRD patterns of (a) ZnO nanorods and (b) MnO_2 nanotubes.

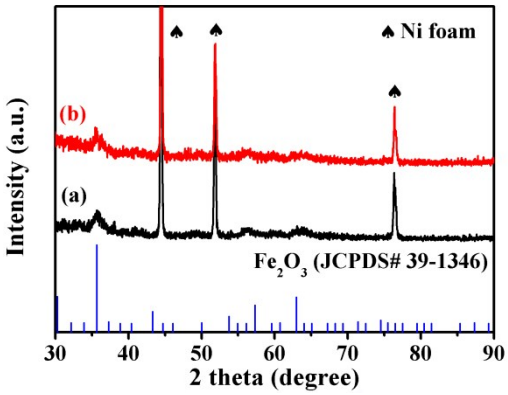

Figure S2. XRD patterns of (a) Fe_2O_3 nanotubes and (b) Fe_2O_3@PPy nanotubes.

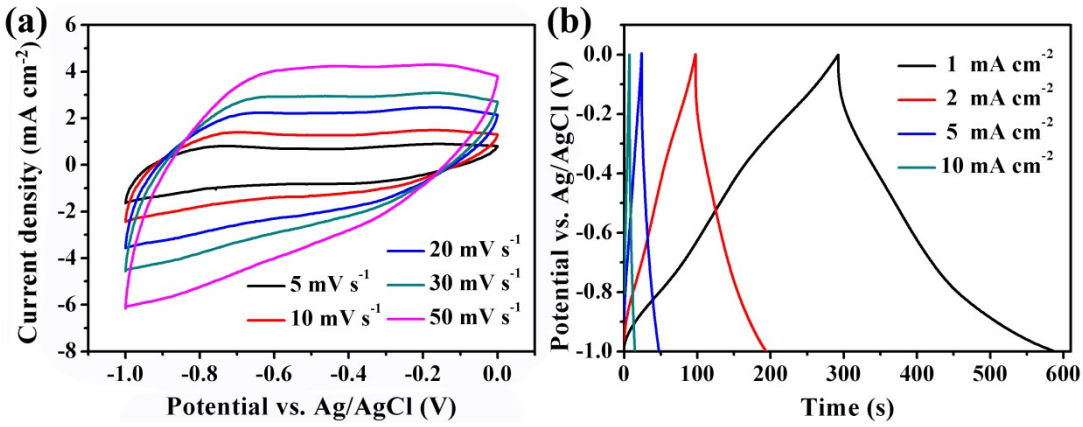

Figure S3. (a) CV curves of Fe_2O_3 nanotubes at varied scan rates; (b) GCD curves of Fe_2O_3 nanotubes at different current densities.

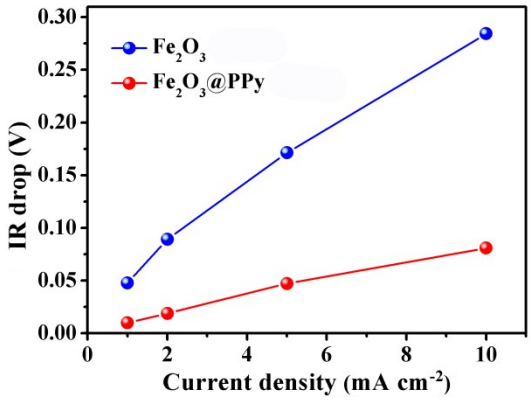

Figure S4. IR drops of Fe_2O_3 nanotubes and Fe_2O_3@PPy nanotubes electrodes at different current densities.

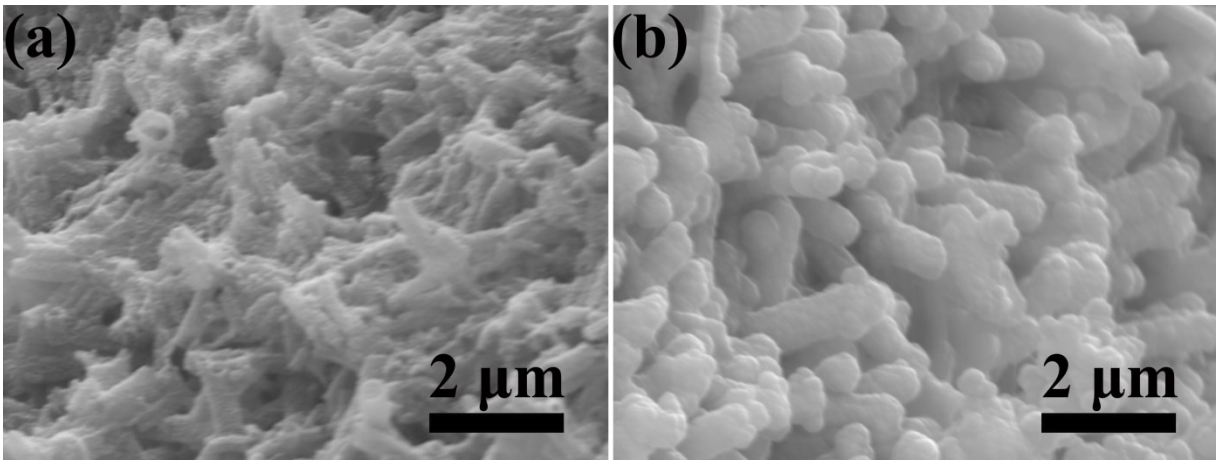

Figure S5. SEM images of (a) Fe_2O_3 nanotubes after 1000 cycles and (b) Fe_2O_3@PPy nanotubes after 5000 cycles in 1 M Na_2SO_4 electrolyte.

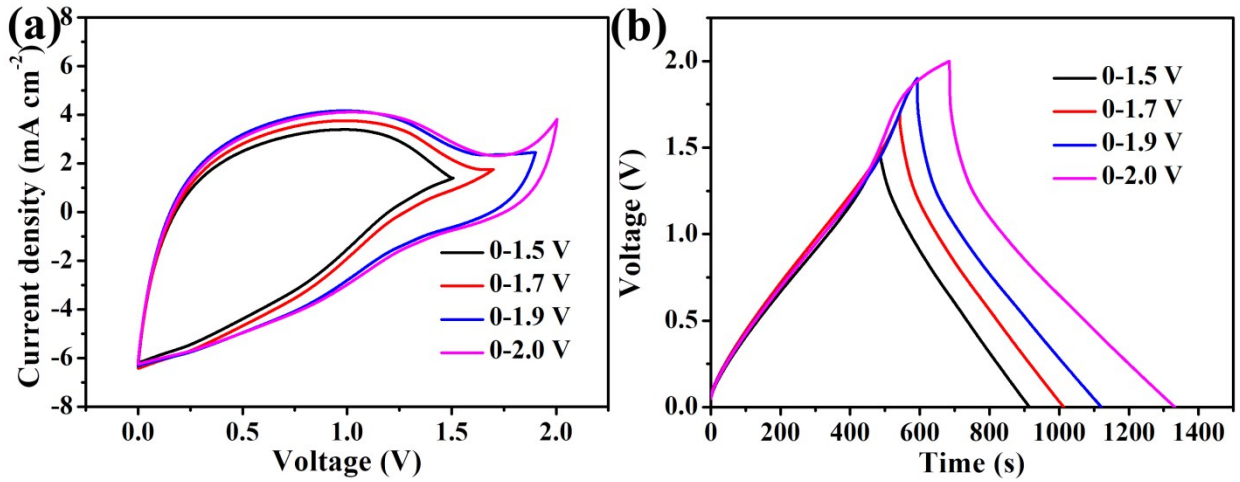

Figure S6. CV curves of the ASC device measured at different operating voltages at scan rate of 10 mV s^{-1}; (b) GCD curves of the ASC device at different operating voltages at a current density of 0.5 mA/cm^2.

Table S1. The specific capacitance of various electrodes in the three-electrode system in references

Electrode materials	electrolyte	Potential window	capacitance	reference
Fe_2O_3 nanotube	1 M Li_2SO_4	-0.8-0.1 V	300 F g^{-1}	[6]
Fe_2O_3@C nanoparticles	1 M Na_2SO_4	-0.5-0.5 V	211.4 F g^{-1}	[7]
Tectorum-likeα-Fe_2O_3/PPy	1 M Na_2SO_4	-0.8-0 V	382.4 mF cm^{-2}	[8]
N-C/Fe_2O_3	5 M LiCl	-0.8-0 V	148.5 mF cm^{-2}	[9]
Tetsubo-like α-Fe_2O_3/C	1 M Na_2SO_4	-1.0-0 V	430.8 mF cm^{-2}	[10]
Fe_3O_4/CNTs	6 M KOH	-1.0-0 V	129 F g-^{1}	[11]
Fe_3O_4/exfoliated graphite	1 M KOH	-1.1-0 V	327 F g^{-1}	[12]
Fe_2O_3@PPy nanotubes	1 M Na_2SO_4	-1.0-0 V	530 mF cm^{-2}	This work
			407 F g^{-1}	

Reference

1. S. Wang, Z. Huang, R. Li, X. Zheng, F. Lu, T. He, *Electrochim. Acta* **2016**, 204, 160-168.
2. P.-Y. Tang, L.-J. Han, A. Genç, Y.-M. He, X. Zhang, L. Zhang, J.R. Galán-Mascarós, J.R. Morante, J. Arbiol, *Nano Energy* **2016**, 22, 189-201.
3. Z. Pan, Y. Jiang, P. Yang, Z. Wu, W. Tian, L. Liu, Y. Song, Q. Gu, D. Sun, L. Hu, In Situ Growth of

Layered Bimetallic ZnCo Hydroxide Nanosheets for High-Performance All-Solid-State Pseudocapacitor, ACS Nano 12 (2018) 2968-2979.

4. Y. Wen, S. Peng, Z. Wang, J. Hao, T. Qin, S. Lu, J. Zhang, D. He, X. Fan, G. Cao, Facile synthesis of ultrathin $NiCo_2S_4$ nano-petals inspired by blooming buds for high-performance supercapacitors, J. *Mater. Chem. A* **2017**, 5 7144-7152.
5. N. Liu, Y. Su, Z. Wang, Z. Wang, J. Xia, Y. Chen, Z. Zhao, Q. Li, F. Geng, *ACS Nano* **2017**, 11, 7879-7888.
6. Y.-G. Lin, Y.-K. Hsu, Y.-C. Lin, Y.-C. Chen, *Electrochim. Acta* **2016**, 216, 287-294.
7. M. Zhang, J. Sha, X. Miao, E. Liu, C. Shi, J. Li, C. He, Q. Li, N. Zhao, *J. Alloys Compd*. **2017**,696, 956-963.
8. L. Wang, H. Yang, X. Liu, R. Zeng, M. Li, Y. Huang, X. Hu, *Ange. Chem. Inte. Ed.* **2017**,56, 1105-1110.
9. W. Fu, E. Zhao, X. Ren, A. Magasinski, G. Yushin, *Adv. Energy Mater.* **2018**, 8 ,1703454.
10. D. Chen, S. Zhou, H. Quan, R. Zou, W. Gao, X. Luo, L. Guo, *Chem. Eng. J.* **2018**, 341, 102-111.
11. D. Guan, Z. Gao, W. Yang, J. Wang, Y. Yuan, B. Wang, M. Zhang, L. Liu, *Mater. Sci. Eng.* B **2013**, 178, 736-743.
12. Z. Sun, X. Cai, Y. Song, X.-X. Liu, *J. Power Sources* **2017**, 359, 57-63.